Anacardic acid induces IL-33 and promotes remyelination in CNS

Åsa Ljunggren-Rose[a,1], Chandramohan Natarajan[a,1], Pranathi Matta[a], Akansha Pandey[a], Isha Upender[a], and Subramaniam Sriram[a,2]

[a]Department of Neurology, Vanderbilt University Medical Center, Nashville, TN 37212

Edited by Lawrence Steinman, Stanford University School of Medicine, Stanford, CA, and approved July 15, 2020 (received for review April 7, 2020)

Given the known neuroreparative actions of IL-33 in experimental models of central nervous system (CNS) injury, we predicted that compounds which induce IL-33 are likely to promote remyelination. We found anacardic acid as a candidate molecule to serve as a therapeutic agent to promote remyelination. Addition of anacardic acid to cultured oligodendrocyte precursor cells (OPCs) rapidly increased expression of myelin genes and myelin proteins, suggesting a direct induction of genes involved in myelination by anacardic acid. Also, when added to OPCs, anacardic acid resulted in the induction of IL-33. In vivo, treatment of with anacardic acid in doses which ranged from 0.025 mg/kg to 2.5 mg/kg, improved pathologic scores in experimental allergic encephalitis (EAE) and in the cuprizone model of demyelination/remyelination. Electron microscopic studies performed in mice fed with cuprizone and treated with anacardic acid showed lower g-ratio scores when compared to controls, suggesting increased remyelination of axons. In EAE, improvement in paralytic scores was seen when the drug was given prior to or following the onset of paralytic signs. In EAE and in the cuprizone model, areas of myelin loss, which are likely to remyelinate, was associated with a greater recruitment of IL-33–expressing OPCs in mice which received anacardic acid when compared to controls.

IL-33 | demyelination | anacardic acid | multiple sclerosis

Oligodendrocytes form extensive processes which wrap around axons and provide the necessary fidelity for the conduction of electrical impulses along the nerves. They also provide key trophic support for the underlying axons and are necessary for axonal integrity (1, 2). Destruction of myelin and the attendant loss of neurological function is a key feature underlying the pathophysiology of demyelinating diseases. These include disorders which are related to underlying infections, autoimmune disorders, or metabolic causes (3–6). Destruction of the myelin sheath slows nerve conduction and eventually leads to destruction of the underlying naked axons. It is well known that protection of the naked axons is necessary to prevent axonal transection and persistent neurological dysfunction (7, 8). Repair and remyelination of naked axons does occur but is often poor or incomplete, which results in permanent neurological deficits (9–11). There is an urgent need to recognize and develop molecules which have the potency to remyelinate axons and thereby improve clinical recovery and restore neurologic function.

Multiple sclerosis (MS) is the prototypic autoimmune demyelinating disease of the central nervous system (CNS) (12). The clinical disability is due to the presumed autoimmune destruction of the myelin membranes and loss of underlying axons. While the acute inflammatory lesions have been managed and treated by a variety of immunomodulatory and immunosuppressive agents, there are currently no treatments to repair and remyelinate axons (13, 14). That is not to say recovery does not happen as a feature of the normal recovery process in MS; it often does, but is ineffective and incomplete, suggesting that existing oligodendrocyte precursor cells (OPCs) could be harnessed to induce remyelination (15).

In our previous study, we have shown that Poly-IC, a known TLR3 agonist, promotes the maturation of OPCs and improves myelination (16). We proposed that one mechanism by which Poly-IC induces the maturation of OPCs was through the induction of IL-33 in glial cells. IL-33 belongs to a family of alarmin molecules and are recognized as first responders to protect the host from invaders. Interestingly, IL-33 has shown to have immunoregulatory functions in autoimmune and inflammatory disease states (17–19). In screening for small molecules, which would induce IL-33 and thereby promote remyelination, we found that inhibitors of histone acetyl transferase (HAT) caused an induction of IL-33. We focused our studies on anacardic acid, a known inhibitor of HAT, and examined its efficacy to induce IL-33 and promote remyelination in experimental models of CNS demyelination.

Results

Treatment of Anacardic Acid Induces Expression of Myelin Basic Protein and Genes Involved in Transcription of Myelin Proteins in OPCs. In vitro treatment of rat OPCs with anacardic acid showed a dose-dependent increase in the induction of myelin basic protein (MBP). Maximal increase of 2.6 ± 0.6-fold over vehicle was seen when 10 μM anacardic acid was added to the culture (Fig. 1 *A* and *B*). We also quantitated the mRNA expression of *Mbp*, along with mRNAs of *Sp1*, *Sox10*, and *Pur*α, in OPCs when cultured with anacardic acid using qRT-PCR. *Sp1*, *Sox10*, and *Pur*α are transcription factors which bind to the promoter region of *Mbp* to initiate gene expression (20). Addition of 5.0 μM anacardic acid resulted in a 7.6 ± 4.08-fold induction of *Mbp* messenger RNA

Significance

Many neurological disorders stem from damage to myelin, the insulating material which wraps around nerves and provides optimal nerve conduction. We previously found that IL-33, a chemical made in response to injury, was able to induce new myelin formation. In exploring compounds which can induce IL-33, we found that anacardic acid, a compound found in the plant kingdom, was able to promote the formation of new myelin. In addition, treatment of mice with anacardic acid induced IL-33 in the nervous system and resulted in reduced injury in animal models of disease in which loss of myelin was experimentally induced. We believe that the actions of anacardic acid warrants further study for the treatment of demyelinating diseases.

Author contributions: Å.L.-R. and S.S. designed research; Å.L.-R., C.N., P.M., A.P., and I.U. performed research; Å.L.-R., P.M., and S.S. analyzed data; and Å.L.-R. and S.S. wrote the paper.

The authors declare no competing interest.

This article is a PNAS Direct Submission.

See online for related content such as Commentaries.

[1]Å.L.-R. and C.N. contributed equally to this work.

[2]To whom correspondence may be addressed. Email: subramaniam.sriram@vumc.org.

This article contains supporting information online at https://www.pnas.org/lookup/suppl/doi:10.1073/pnas.2006566117/-/DCSupplemental.

First published August 17, 2020.

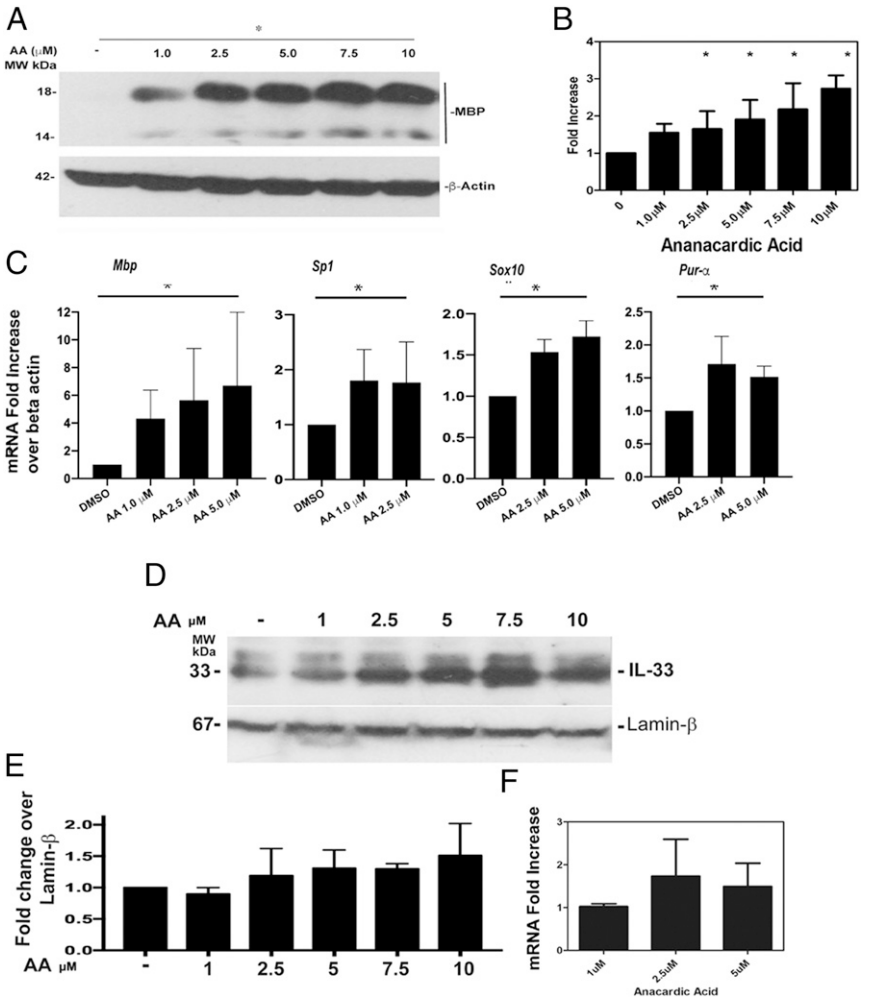

Fig. 1. Induction of myelin proteins in rat OPCs cultured with anacardic acid. Western blot showing a dose–response induction of MBP with anacardic acid (*A*); quantitation of Western blot expression levels of MBP after normalizing with beta actin (*B*); qPCR results of expression of *mbp, sp-1*, *sox10*, and *pur alpha* following culture of OPCs with anacardic acid (*C*); Western blot analysis on the expression of IL-33 protein in OPCs cultured with anacardic acid (*D*); quantitation of expression of IL-33 protein and normalization with beta lamin (*E*); and qPCR analysis on the induction of IL-33 in OPCs cultured with anacardic acid (*F*). All experiments were repeated a minimum of three times. $*P < 0.02$ compared to controls.

(mRNA) when compared with vehicle-treated controls. We also observed a 2.29 ± 0.52-fold increase in *Sp1*, 1.86 ± 0.13-fold increase in *Sox10*, and 1.63 ± 0.11-fold increase in *Pur*α (Fig. 1*C*). All results are expressed as ±SD.

In Vitro Treatment of OPCs with Anacardic Acid Increases Intracellular IL-33. We examined the ability of anacardic acid to induce the expression of IL-33 using Western blot assays. In a summary of three separate experiments, we observed a 1.6 ± 0.4-fold increase in the expression of IL-33 in nuclear extract of OPCs cultured with the addition of 10 μM anacardic acid. Expression of mRNA of IL-33 was also increased with maximal induction of 1.8 ± 0.4 seen with addition of 2.5 μM anacardic acid (Fig. 1 *D–F*).

Anacardic Acid Induces Differentiation of Rat OPCs. During the period of differentiation, OPCs in culture stop dividing and the cell processes show extensions coupled with increased expression of MBP. When compared with the vehicle (DMSO)-treated control cells, addition of 5 μM anacardic acid to the cultures resulted in increased extension of the cellular processes and a 2.1-fold increase in the expression of MBP (Fig. 2 *A–D*).

Anacardic Acid Treatment Attenuates the Clinical and Pathological Scores in Experimental Allergic Encephalitis. We examined the clinical severity of animals induced to develop experimental allergic encephalitis (EAE) and treated with anacardic acid. A summary of four different experiments were performed using four different doses and treatment regimens of anacardic acid and its effect on the clinical paralytic scores and the amount of demyelination was determined. In animals which received 2.5 mg/kg anacardic acid beginning from day 0 and treated daily through day 25, 5/15 animals developed paralytic signs, mean paralytic score of 1.1 ± 0.4. In animals which received DMSO, 18/20 animals became paralytic, with a mean severity score of 2.4 ± 0.4. Reduction of clinical paralysis was also present when anacardic acid at doses of 0.25 and 0.025 mg/kg was given throughout the period of study. The mean maximal clinical severity in animals which received 0.25 mg/kg was 1.1 and 0.8 in animals which received a dose of 0.025 mg/kg ($P < 0.01$ for the above dosing regimens compared to DMSO). When a dose of 0.0025 mg/kg anacardic acid beginning day 0 was given, the mean maximal paralytic score was 2.3, which was similar to scores seen in animals treated with vehicle. However, there was a 4-d delay

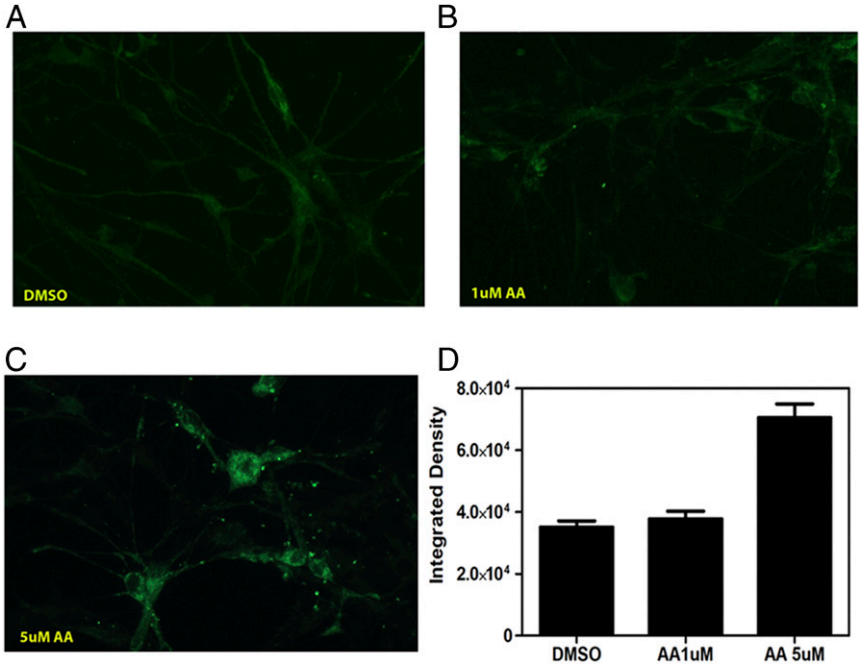

Fig. 2. (*A–C*) Immunofluorescence analysis of MBP expression in OPCs treated with anacardic acid for 10 d in vitro. (*D*) Quantitation of MBP expression in OPCs.

in the animals to reach maximal disease severity when compared to mice treated with DMSO (Fig. 3*A*).

To determine if delaying the treatment regimen will alter the course of EAE, we began treatment at day 11 when the earliest clinical paralytic signs were evident. Among the 10 animals in the DMSO group, 7/10 continued to show paralytic signs on day 20 with a mean paralytic score of 1.8 ± 0.6. In the animals which received anacardic acid, only one animal in each of 2.5 mg/kg and 0.25 mg/kg treatments (2/10) failed to improve and each animal in these groups showed grade 1 paralysis (Fig. 3*B*).

To further examine the effect of anacardic acid on CNS demyelination, spinal cord sections obtained from cervical, thoracic, and thoracolumbar regions were stained with Luxol Fast Blue (LFB) and the amount of demyelination quantitated. The demyelinated regions were marked out and the percent demyelination was calculated as a ratio of demyelinated regions compared to total white matter of the spinal cord. In mice which received 2.5 mg/kg anacardic acid starting at day 0, there was a 2.3 ± 1.1% decrease in the myelinated areas. In the group which received DMSO, there was a 9.9 ± 4.9% decrease in the myelinated regions (P,0.01). Demyelination was not seen in the 5 animals which received either 0.25 mg/kg or 0.025 mg/kg anacardic acid. In the animals which received anacardic acid beginning from day 11 postimmunization, there was 7.4 ± 4.7% decrease in myelinated areas in the DMSO group and 2.4 ± 2.0% in the group that received 2.5 mg/kg anacardic acid ($P < 0.02$) (Fig. 3*C*).

Since MOG p35-55–induced EAE is a T cell-mediated disease caused by the activation of IL-17+ autoreactive T cells, we explored the possibility that anacardic acid could interfere with activation and proliferation of MOG p35-55–activated T cells. In the *SI Appendix* shown, addition of anacardic acid to MOG p35-55–primed T cells did not inhibit either T cell proliferation nor did it reduce the production of IL-17 or IL-2 when compared to vehicle-treated cells (*SI Appendix*, Tables S1 and S2 and Fig. S1).

Improved Remyelination in Animals Receiving Cuprizone and Treated with Anacardic Acid. Cuprizone is a copper chelating agent and when added to the diet induces extensive demyelination in large white matter tracts and is best seen in the corpus callosum. Demyelination reaches a peak after animals are fed with the special diet for 4–6 wk (21). Prior studies have shown that withdrawal of cuprizone in the diet results in rapid remyelination of axons (22–24). Demonstration of a therapeutic effect will have to show that the drug is better than what would otherwise occur naturally. In order to overcome the problem with rapid remyelination seen when the cuprizone is withdrawn from the diet, we continued with cuprizone in the diet for a total period of 9 wk. Mice were treated with either anacardic acid 5 mg/kg, 2.5 mg/kg, or 1.25 mg/kg or vehicle along with cuprizone containing chow beginning at week 6 and continuing treatment until week 9.

Improvement in myelination was seen at the end of 9 wk when compared to vehicle treated controls (Fig. 4). When compared to naïve mice, animals which received anacardic acid showed 77.7 ± 7.3% staining of the corpus callosum with anti-MBP antibody and 61.73 ± 7.6% staining with anti-MOG (Fig. 4*B*). In mice treated with vehicle, there was 58.04 ± 14.1% staining with anti-MBP antibody and 40.70 ± 11.5% staining with anti-MOG. ($P <$ 0.01). Analysis of remyelination at week 7 and 8 (animals which received 1 to 2 wk on anacardic acid) showed no differences in the expression of myelin staining with LFB when compared to controls, suggesting that at least 3 wk of treatment with anacardic acid was needed (*SI Appendix*, Fig. S3). There was no difference in LFB staining at week 9 between the different doses of anacardic acid used for treatment (*SI Appendix*, Fig. S2).

To quantify remyelination, we performed electron microscopy (EM) studies on the myelination of axons in the corpus callosum on animals fed with diet containing 0.3% cuprizone and treated with vehicle, 2.5 mg/kg anacardic acid, or 0.25 mg/kg anacardic acid from week 6 to week 9. A total of 150 axons were examined, and the ratio of the inner diameter of the axon to the diameter for the axon (including the myelin sheath) and expressed as the g ratio was calculated for each axon. The g ratio in the animals which received 2.5 mg/kg anacardic acid was 0.663 ± 0.06, and

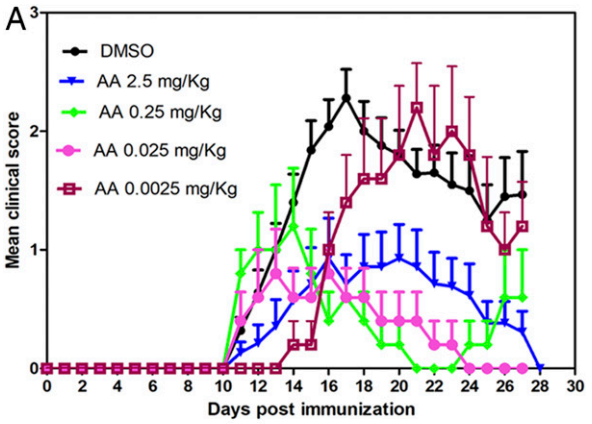

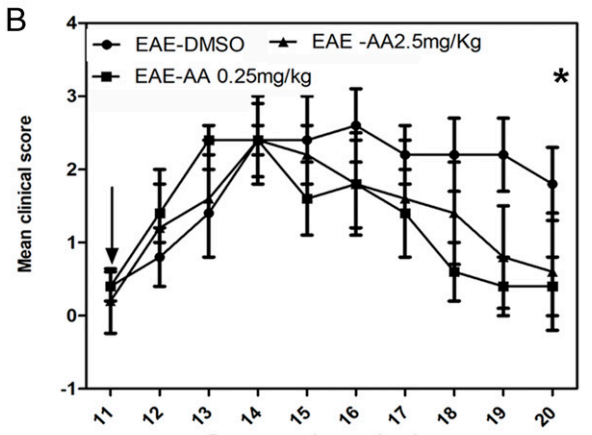

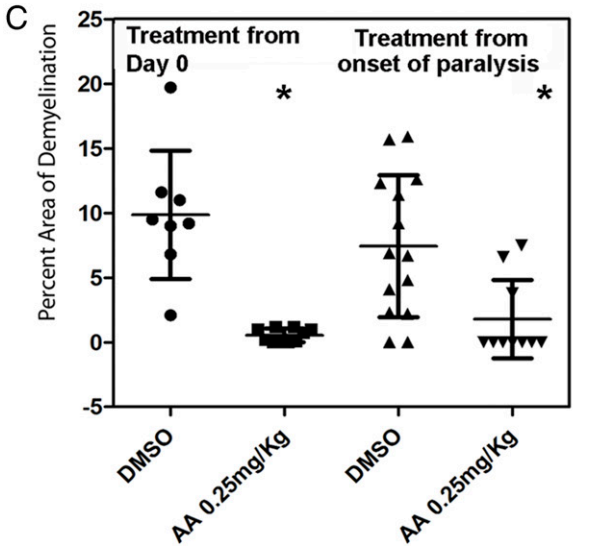

Fig. 3. Effect of anacardic acid on development and progression of EAE. (*A*) Paralytic scores in animals induced to develop EAE and treated with anacardic acid from day 0 of immunization. Paralytic scores of animals with treatment begun on day of onset of signs of paralysis (*B*) and quantitation of demyelination as assessed by staining with LFB in animals from at least two noncontiguous areas of spinal cord from each animal (*C*). The data are represented as the percent decrease in the myelinated regions of the white matter tracts of the spinal cord. $*P < 0.01$ anacardic acid compared to vehicle.

this value was lower than in mice that received 0.25 mg/kg (mean g ratio, 0.69 ± 0.09), indicating better remyelination at the higher dose of anacardic acid (Fig. 4 *D–F*). Both doses of anacardic acid were superior to vehicle-treated control. In animals which were treated with vehicle alone, the g ratio was 0.71 ± 0.08 ($P < 0.0001$ one-way ANOVA).

Increased Expression of IL-33 in CNS Models of Demyelination. To examine the role of IL-33 in demyelination/remyelination, we examined the expression of IL-33 in regions of demyelination in animals fed cuprizone or induced to develop EAE and treated with anacardic acid. In cuprizone-treated mice, there was a marked increase in the expression of IL-33 in the corpus callosum of mice when compared to vehicle-treated mice. When IL-33 was measured, the integrated cell density was increased by 22.2% in anacardic acid-treated animals over vehicle-treated controls. Direct counting of number of IL-33–positive cells showed a 47.2.2% increase in anacardic acid-treated animals compared to naive mice treated (Fig. 5, $P < 0.01$). The IL-33–positive cells colocalized with cells stained with anti-Olig2 antibody. IL-33 was not seen in GFAP-expressing astrocytes or in microglial cells stained for CD68 (*SI Appendix*, Fig. S4).

We next compared the expression of IL-33 in areas of myelin loss in anacardic acid-treated mice with those treated with DMSO in animals induced to develop EAE. We sampled 12 areas from 5 animals that received anacardic acid (2.5 mg/kg group), which showed the presence of demyelinating lesions, and compared them with those that received DMSO. Each section was stained with anti-MBP and anti-IL-33 antibodies, the images were merged and the number of IL-33–staining cells were counted in demyelinated regions (Fig. 6). In anacardic acid-treated animals, there were more IL-33+ cells within the demyelinated regions when compared to vehicle-treated controls. In the latter group, the IL-33+ cells were located in the normal appearing matter at the edge of the demyelinated regions. The mean number of IL-33–expressing cells within the demyelinated region covering 100^3 pixels was 4.5 ± 0.6 in the anacardic acid-treated animals and 2.7 ± 1.08 in the untreated group ($P < 0.02$). All of the IL-33–expressing cells colocalized in cells stained with anti-Olig2 antibody, suggesting that the majority of IL-33 were present in oligodendrocytes.

Discussion

Our studies demonstrate that anacardic acid improved remyelination and reduced the extent of demyelination in two separate models of demyelination/remyelination. The improvement in the pathological scores was accompanied by an increase in the number of IL-33–expressing Olig2+ cells in the areas of myelin loss. Our studies demonstrating remyelination using electron microscopy was performed in the cuprizone model, since the location of demyelination in this model, and unlike that with EAE, occurs in anatomically determined sites, allowing for comparison between treatment groups. The dose-dependent improvement in g ratios suggests increased remyelination following treatment with anacardic acid. Our treatment protocol used in the cuprizone model is different from other studies wherein remyelination was examined following withdrawal of cuprizone. In our studies, improvement in myelination scores was seen when animals were continually fed with cuprizone and treated with anacardic acid, suggesting that anacardic acid can overcome the ongoing gliotoxic effects of cuprizone (22, 23). We suggest two overlapping mechanisms of myelin gene expression in OPCs induced by anacardic acid: a direct action of anacardic acid on myelin gene expression and an indirect process mediated through the induction of IL-33 (*SI Appendix*, Fig. S5).

Anacardic acid, a product from the cashew tree (*anacardium occidentale*), was noted to be a histone acetyl transferase (HAT)

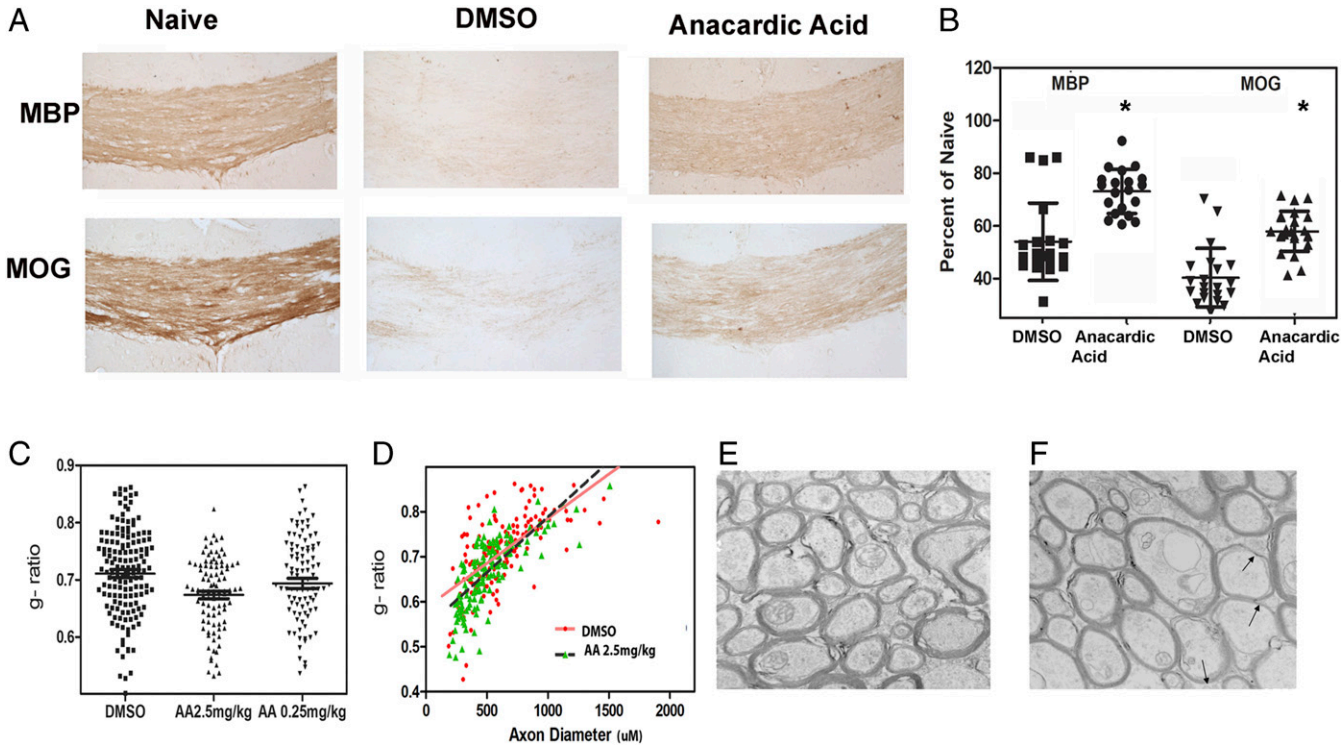

Fig. 4. (*A*) Enhanced remyelination in mice treated with anacardic acid and stained with MBP or MOG. (*B*) Quantitation of MBP and MOG expression from eight animals in the treated group and an equal number of controls (*$P < 0.01$ myelin antigen staining in anacardic acid treated compared to DMSO). (*C–F*) EM analysis of remyelination in cuprizone-fed mice treated with anacardic acid. Sagittal section of corpus callosum as stained by osmium tetroxide and the g ratio manually calculated on 150 axons. Distribution of g ratio between anacardic acid treated and DMSO-treated mice ($P < 0.001$ ANOVA) (*C*), scatter plot showing the difference in the slope between anacardic acid-treated and vehicle-treated mice (*D*), and sections of axons in anacardic acid-treated animals (*E*) and vehicle-treated animals (*F*). Arrows show the thinning of myelin sheath of axons in vehicle-treated mice.

inhibitor (24, 25). Structurally it is an organic compound consisting of salicylic acid substituted with a saturated 15-carbon alkyl side chain. In view of its ability to influence epigenes, the compound has been explored as treatment for neoplastic conditions. Since it has inhibitory effects on activation of NFkb and matrix metalloproteases, its role in reducing tissue inflammation cannot be excluded and may provide a basis for its therapeutic effect in EAE (25). However, the ability of anacardic acid to induce differentiation of oligodendrocytes and improve measures of remyelination is novel. Since anacardic acid has been known to regulate a number of enzymatic pathways, it is not known if these pathways overlap with those that have been described to promote remyelination (26–28).

The cuprizone-induced demyelination and the MOG p35-55 EAE models differ in the mechanism of glial injury. While EAE is thought to result from the actions of antigen-primed T cells on glial cells, cuprizone model of demyelination is primarily gliotoxic and does not require T cell activation. Further, anacardic acid did not suppress T cell proliferation or inflammatory cytokine expression levels, suggesting that the compound may act by reducing injury and promoting repair.

IL-33 is a tissue-derived nuclear cytokine belonging to the IL-1 family with important role in tissue repair, in the regulation of type 2 immunity and in response to inflammation (17, 29–31). While located in the nucleus, it is released into the extracellular space following cell death. Like IL-1a, IL-33 localizes to the nucleus and binds chromatin through a common chromatic binding motif (17, 19, 32). Nuclear functions of IL-33 in transcriptional regulation has been proposed, but they have not included transcription of myelin genes (33).

Prior studies have suggested an immunoprotective role of IL-33 following CNS injury. IL-33 is recognized as one of the "alarmins" and thought to play a role in host defense. Hence, IL-33 is expressed at high levels at entry points of putative pathogens and are presumed to detect "danger" (34). It is also expressed at high levels in the CNS and mostly in oligodendrocytes. Since the CNS is not a direct portal of entry for pathogens, the role of IL-33 as an "alarmin" in CNS is less clear (35). However, a number of observations suggest a neuroreparative role for IL-33 in the CNS. In vivo administration of IL-33 reduces the severity of EAE when given after the development of paralytic signs and administration of anti-IL-33 antibody increases clinical severity scores (36). IL-33 receptor-deficient mice also showed worse clinical scores in mice induced to develop EAE. Also, in vivo administration of IL-33 improves the myelin content in regions of spinal cord following spinal cord trauma, suggesting its protective role in noninflammatory disorders (32). These studies therefore suggest that IL-33 may function to protect oligodendrocytes and repair myelin injury, and both endogenous nuclear IL-33 and exogenous forms are effective in improving recovery from tissue injury. Although the mechanism by which IL-33 promotes recovery is not clear, it is thought to skew immune response to the M2 phenotype in microglial cells, which has been shown to reduce inflammatory injury (37). Our studies show that in addition, IL-33 can directly influence MBP expression and promote remyelination. IL-33–mediated therapeutic strategies do not sort out the role of nuclear IL-33, when compared to extracellular IL-33, in promoting neural repair. Exogenous addition of IL-33, in mice with genetic deletion of the IL-33R or the knockdown of the IL-33 gene, are associated with increased severity of EAE, suggesting that the nuclear and extracellular signaling may be beneficial in remyelination.

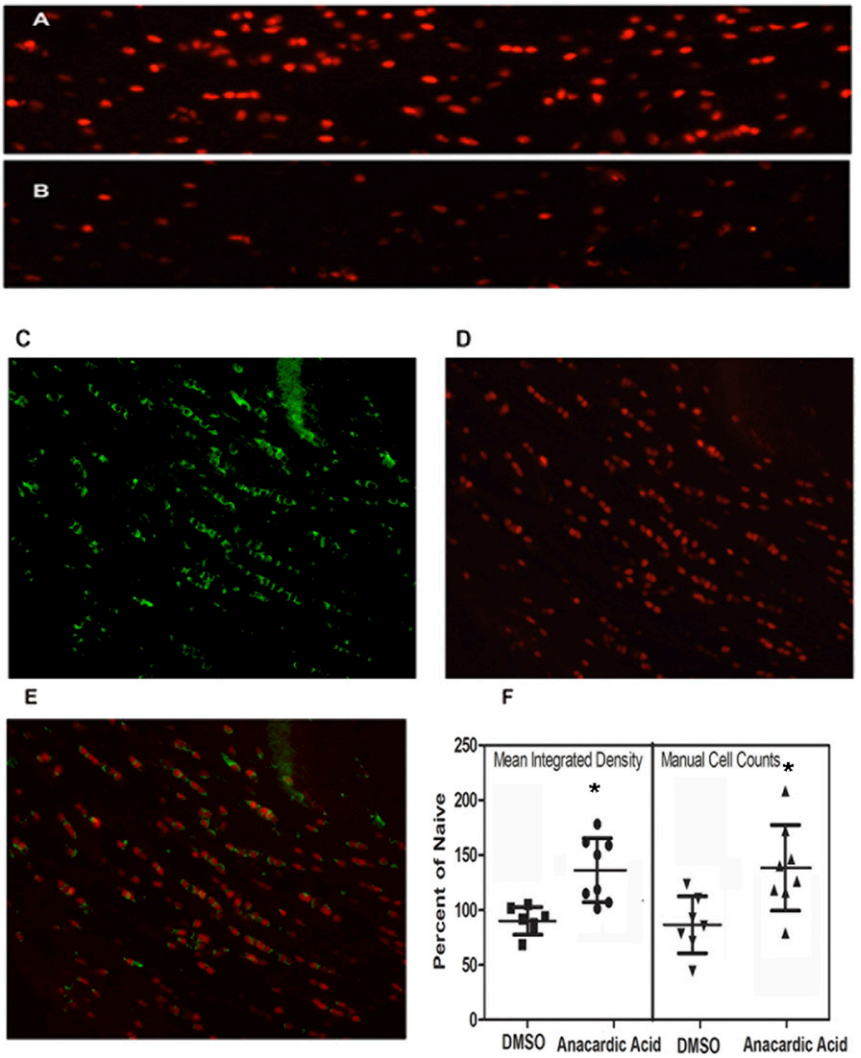

Fig. 5. (*A–C*) Colocalization of IL-33–staining cells in corpus callosum of mice fed cuprizone. IL-33 in corpus callosum of anacardic acid treated mice (*A*) and corpus callosal regions showing reduced number of IL-33–expressing cells in vehicle-treated animals (*B*). Oligodendrocytes stained with anti CC-1 antibody (*C*), staining of cells with anti-IL-33 antibody (*D*), and colocalization of the staining of IL-33 in CC-1–positive cells (*E*). (*F*) Quantitative analysis of IL-33 expression in corpus callosum in treated and untreated mice (*$P < 0.01$).

One of the approaches to improve remyelination have focused on inducing the proliferation and differentiation of resident oligodendrocyte precursor cells in the region around the area of demyelination (27). These include monoclonal antibodies directed against Lingo1, which has shown to increase OPC differentiation and maturation (38–40). Other small molecules directed against the muscarinic receptor, antihistamine agents, and antifungal agents demonstrate a common pathway for myelin gene expression (41–43). In phase II clinical studies, the effect of remyelination has been modest and, hence, the entry of these compounds to phase III trials are at present uncertain (44, 45).

The ability of anacardic acid to induce oligodendrocyte maturation directly and indirectly through induction of IL-33 and its trophic effects on axons suggests that the compound offers therapeutic promise in the treatment of human demyelinating disease such as MS.

Materials and Methods

Reagents. Antibodies specific for MBP (sc-13914, sc-271524), β-Actin (sc-47778), and Lamin-β (sc-6216) were obtained from Santa Cruz Biotechnologies. IL-33 antibodies were purchased from Enzo (ALX-804-840) and R&D Systems (AF3626). Antibodies specific for CC1 (ab16794), GFAP (ab7260), and CD68 (ab125212) were purchased from Abcam. Olig2 antibody (AB9610) was obtained from Millipore. TRIzol, SuperScript VILO cDNA kit, PowerUp SYBR Green master mix solution, Alexa-488, Alexa-555, and Alexa-594 conjugated secondary antibodies were purchased from Thermo Fisher Scientific. Anacardic acid was purchased form Selleck Chemicals. Triton X-100, mammalian protease inhibitor mixture, and DNase I from bovine pancreas were purchased from Sigma. Percoll solution was purchased from GE Healthcare Biosciences. Cuprizone [oxalic acid bis (cyclohexylidene hydrazide)] containing chow diet was purchased from Envigo. PDGF and basic FGF were purchased from Peprotech Inc. MOG35-55 immunization kit (EK-2110) was procured from Hooke Laboratories (Lawrence, MA). OPC differentiation media was purchased from Sciencell.

Animals. Male and female C57/B6 mice 8–12 wk of age were obtained from Jackson Laboratories. Sprague–Dawley rats were obtained from Charles River Laboratories. All experimental procedures involving animals were carried out in accordance with the recommendations in the NIH Guide for the Care and Use of Laboratory Animals (46). The institutional animal care and use committee of Vanderbilt University Medical Center (protocol M1700140-00; M1600127-00) approved the study. All animals were housed in temperature- and humidity-controlled rooms maintained on a 12-h dark/light cycle. Animals were

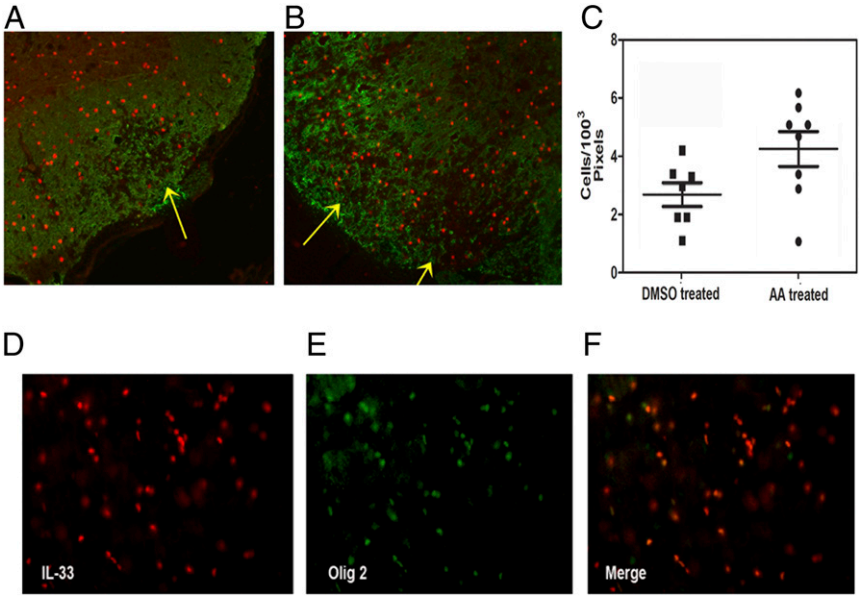

Fig. 6. Colocalization of IL-33–expressing cells with Olig2-expressing oligodendrocytes. (*A*–*C*) Double staining for MBP and IL-33 in spinal cord sections of five animals with EAE and treated with anacardic acid (2.5 mg/kg) or five animals treated with DMSO. DMSO treated (*A*), anacardic acid treated (*B*), and quantitation of IL-33 staining cells within the demyelinated regions (*C*). Note the increased expression of IL-33–positive cells in the demyelinated regions in mice treated with anacardic acid. Arrows show the region of demyelination in the lateral column of the spinal cord. Axial sections of spinal cord stained with anti-IL-33 antibody (*D*), and sections stained with anti-Olig2 antibody (*E*). (*F*) Merged section showing the colocalization of IL-33 with Olig2. Most of the cells expressing Olig2 also express IL-33.

euthanized using CO_2 narcosis. All efforts were made to minimize the number of animals used and to ameliorate their suffering.

Preparation of Oligodendrocyte Precursor Cells. Two-day-old newborn pups from pregnant mothers were used for the isolation of OPCs. Rat OPCs were purified from cerebral hemispheres following previously published protocol. Briefly, 2-d-old Sprague–Dawley rat pups were decapitated, brains excised, and meninges-free cerebral hemispheres were collected and processed as described by us previously. Using this method, we have previously shown that >95% of cells belong to one of three groups, A2B5$^+$, Olig2$^+$MBP$^-$, and O4$^+$MBP$^+$ (47).

Cuprizone-Induced Demyelination. Eight- to nine-week-old C57/B6 mice were fed with chow containing 0.2 or 0.3% cuprizone for 9 wk. Once every third day, old cuprizone containing chow was replaced with fresh chow. From week 6 onwards, until the end of the experiment, mice were treated daily with different doses of anacardic acid in 0.1 mL containing 15% DMSO or vehicle alone. At the end of the ninth week, mice were euthanized and perfused with 4% paraformaldehyde in phosphate buffered saline (PBS). Whole brains were collected and embedded in paraffin blocks for histological analysis.

Experimental Autoimmune Encephalomyelitis. Ten- to thirteen-week-old female C57/B6 mice were immunized with MOG_{35-55} peptide emulsion containing complete Freund's adjuvant. Pertussis toxin (100–150 ng dose calculated based on the potency of the lot) was injected intraperitoneal (i.p.) once on the day of immunization and 24 h later. Mice received anacardic acid in 15% DMSO from the day of immunization or from the onset of paralytic signs. The paralytic scores were as follows: 0, normal; 1, loss of tail tone; 2, weakness of hind limbs with inability to right; 3, paresis of hind limbs; 4, paralysis of hind and fore limbs; 5, death. Paralytic scores were recorded daily. After the experimental period, mice were anesthetized and perfused with 4% paraformaldehyde in PBS, and spinal cords were collected and stored in 4% paraformaldehyde solution. Spinal cords were then decalcified, sections were embedded in paraffin blocks, and subjected to histological analysis.

Western Blot Analysis. Western blot studies were performed from OPC cultures as previously described (16). Briefly stated, OPCs obtained from 2- to 3-d-old rat pup brains were cultured with increasing doses of anacardic acid or vehicle for 10 d in differentiation medium. At the end of the culture period, cell and nuclear isolates were prepared and the proteins separated on 10% SDS gels and probed for the presence of MBP or IL-33 using anti-MBP or anti-IL-33 antibody using enhanced chemiluminescent (ECL) reagents. β-actin for cytosolic proteins and lamin-β for nuclear proteins were used as loading controls and probed with respective antibodies. Images of Western blot bands were scanned and the densitometric analysis of bands were quantified using ImageJ software.

Quantitative Real-Time PCR. qRT-PCR analysis was performed in postnatal 3- or 4-d-old OPCs (3×10^6) treated with either DMSO vehicle or anacardic acid for 4 h at 37 °C to examine the expression of myelin-related genes and known transcription factors that bind at the *Mbp* promoter region. After the incubation, cells were washed with PBS and lysed with TRIzol reagent, and total RNA was isolated following manufacturer's instructions. Complimentary DNA was synthesized from total RNA using SuperScript VILO cDNA kit. qRT-PCR was performed using PowerUp SYBR-Green master mix solution in The Bio-Rad CFX Real-Time PCR instrument. Data were analyzed using Bio-Rad CFX manager version 3.1 software. Details of the PCR primers are shown in *SI Appendix*, Table S1.

Immunocytochemistry. To examine the expression of MBP using immunohistochemical methods, OPCs were harvested and cultured as outlined for Western blot studies. Once every 3 d, anacardic acid at different doses (in differentiation media) were replaced. After 10 d of culture with anacardic acid, cells were fixed with 4% paraformaldehyde in PBS for 20 min at room temperature. Cells were washed 2×5 min with 0.1 M Tris pH 8, 3×5 min with PBS and permeabilized with 0.5% Triton X-100 for 15 min at room temperature. Cells were washed 1×3 min with PBS and blocked in 0.03% Triton X-100 and 10% bovine serum in PBS for 1 h at room temperature. Staining was performed using anti-MBP mouse monoclonal antibody (1:50 dilution) in blocking solution, and the chamber slides were incubated overnight (16–18 h) at 4 °C. The next day, wells were washed 3×5 min with PBS containing 0.3% Triton X-100 and 2% bovine serum. Cells were incubated with secondary antibodies (Alexa 488-conjugated donkey anti-mouse) at 1:500 dilution in blocking solution for 2 h at room temperature. Chambers were washed 3×5 min with washing buffer and mounted using DAPI mounting medium and examined using a fluorescence microscope (Olympus Ax70A)

with a charge-coupled device (CCD) camera (Q color 3, Olympus, USA), and ImageJ software was used to analyze the fluorescent staining.

Immunohistochemistry. Paraffin-embedded brain tissue and spinal cord tissue were cut with serial coronal sections (8 μm thickness) and were subjected to histochemical staining with LFB. For immunostaining, sections were deparaffinized, and antigen retrieval was performed using antigen retrieval solution (Enzo, pH 9) for 20 min in an autoclave. Sections were washed for 5 min with water, and slides were processed for chromagen horseradish peroxidase staining using the Multiview PLUS kit from ENZO according to manufacturer's recommendations. For fluorescent staining, slides were washed for 5 min with Enzo wash buffer and incubated with respective primary antibodies diluted in Enzo wash buffer (anti CC-1, anti-GFAP, anti-CD68, anti-Olig2, anti-IL-33, anti-MBP, and anti-MOG antibodies) for 1 h at room temperature. Sections were washed 3 × 5 min with wash buffer and incubated with Alexa 488- or 594-conjugated secondary antibodies (1:500) for 1 h at room temperature. After washing sections 4 × 5 min, the sections were mounted using DAPI mounting medium. The stained sections were imaged using a microscope (Olympus Ax70A), and ImageJ software was used to analyze the chromagen and the fluorescent staining.

Image Analysis for EAE Spinal Cord Tissue. For estimating the amount of demyelination in the spinal cords of mice with EAE, a minimum of two sections of the spinal cord from each animal was examined. The regions of demyelination (loss of LFB staining) and total area of white matter tracts (without the central gray) in the axial sections was outlined in each section and the data expressed as the percent decrease in area of myelination compared to the total area of nongray regions of the cord and was done by two blinded independent readers (48).

Image Analysis for Cuprizone-Treated Animals. To quantify the amount of myelin staining in anacardic acid-treated animals compared to vehicle controls, both MBP and MOG antibodies were used in immunostaining. Identical imaging parameters were set for all slides. Magnification (10×) was acquired and three images of the corpus callosum were taken, which included the central body and the regions of the cornua on each side. Images were converted to 8-bit and inverted, and the mean pixel intensities (representing the white areas) were acquired and compared to naïve. To quantify number of IL-33–positive cells, central body corpus callosum (representing an 1,800 × 399 pixel area) was analyzed and counted manually by two independent readers and compared to naïve control.

EM Analysis. Mice were perfused with 2% paraformaldehyde, 2% glutaraldehyde in 0.1 M cacodylate, and sagittal sections of the brain was made. The samples were further fixed in 2.5% glutaraldehyde for 24 h, postfixed in 1% OsO_4 and stained with 1% uranyl acetate. The brain slices were then dehydrated in a graded ethanol series and infiltrated with Epon-812 using propylene oxide as a transition solvent. The Epon-812 was polymerized at 60 °C for 48 h and sectioned on a UC7 ultramicrotome at a nominal thickness of 70 nm. TEM was performed using FEI Tecnai T12 operating at 100 kV using an AMT CCD camera. The ratio of diameter of axon to the area of the nerve including the myelin was manually measured and the g ratio was determined using published methods (49).

Statistical Analysis. All data are presented as mean ± SD. Comparisons between treatment groups versus controls were analyzed by Student's unpaired *t* test. EAE and EM data were analyzed with one-way ANOVA comparison. Statistical analysis was performed using Prism 8 (GraphPad Software), and *P* value less than 0.05 was considered statistically significant.

Data Availability. All data, associated protocols, methods, and sources of materials are available in the main text or in *SI Appendix*.

ACKNOWLEDGMENTS. Dr. Sriram was supported by the William Weaver III and Dr. Tom West fund.

1. K. A. Nave, B. D. Trapp, Axon-glial signaling and the glial support of axon function. *Annu. Rev. Neurosci.* **31**, 535–561 (2008).
2. J. R. Plemel, W. Q. Liu, V. W. Yong, Remyelination therapies: A new direction and challenge in multiple sclerosis. *Nat. Rev. Drug Discov.* **16**, 617–634 (2017).
3. R. M. Stassart, W. Möbius, K. A. Nave, J. M. Edgar, The axon-myelin unit in development and degenerative disease. *Front. Neurosci.* **12**, 467 (2018).
4. E. G. Hughes, S. H. Kang, M. Fukaya, D. E. Bergles, Oligodendrocyte progenitors balance growth with self-repulsion to achieve homeostasis in the adult brain. *Nat. Neurosci.* **16**, 668–676 (2013).
5. G. J. Duncan *et al*., Myelin regulatory factor drives remyelination in multiple sclerosis. *Acta Neuropathol.* **134**, 403–422 (2017).
6. R. J. M. Franklin, C. Ffrench-Constant, Regenerating CNS myelin - from mechanisms to experimental medicines. *Nat. Rev. Neurosci.* **18**, 753–769 (2017).
7. Y. Lee *et al*., Oligodendroglia metabolically support axons and contribute to neurodegeneration. *Nature* **487**, 443–448 (2012).
8. B. D. Trapp *et al*., Axonal transection in the lesions of multiple sclerosis. *N. Engl. J. Med.* **338**, 278–285 (1998).
9. R. J. Franklin, Why does remyelination fail in multiple sclerosis? *Nat. Rev. Neurosci.* **3**, 705–714 (2002).
10. M. R. Kotter, A. Setzu, F. J. Sim, N. Van Rooijen, R. J. Franklin, Macrophage depletion impairs oligodendrocyte remyelination following lysolecithin-induced demyelination. *Glia* **35**, 204–212 (2001).
11. J. M. Frischer *et al*., Clinical and pathological insights into the dynamic nature of the white matter multiple sclerosis plaque. *Ann. Neurol.* **78**, 710–721 (2015).
12. A. Compston, A. Coles, Multiple sclerosis. *Lancet* **372**, 1502–1517 (2008).
13. L. Wooliscroft, E. Silbermann, M. Cameron, D. Bourdette, Approaches to remyelination therapies in multiple sclerosis. *Curr. Treat. Options Neurol.* **21**, 34 (2019).
14. K. L. H. Cole, J. J. Early, D. A. Lyons, Drug discovery for remyelination and treatment of MS. *Glia* **65**, 1565–1589 (2017).
15. J. W. Prineas, F. Connell, Remyelination in multiple sclerosis. *Ann. Neurol.* **5**, 22–31 (1979).
16. C. Natarajan, S. Y. Yao, S. Sriram, TLR3 agonist poly-IC induces IL-33 and promotes myelin repair. *PLoS One* **11**, e0152163 (2016).
17. F. Y. Liew, N. I. Pitman, I. B. McInnes, Disease-associated functions of IL-33: The new kid in the IL-1 family. *Nat. Rev. Immunol.* **10**, 103–110 (2010).
18. M. Milovanovic *et al*., IL-33/ST2 axis in inflammation and immunopathology. *Immunol. Res.* **52**, 89–99 (2012).
19. J. Schmitz *et al*., IL-33, an interleukin-1-like cytokine that signals via the IL-1 receptor-related protein ST2 and induces T helper type 2-associated cytokines. *Immunity* **23**, 479–490 (2005).
20. A. Tretiakova, A. Steplewski, E. M. Johnson, K. Khalili, S. Amini, Regulation of myelin basic protein gene transcription by Sp1 and Puralpha: Evidence for association of Sp1 and Puralpha in brain. *J. Cell. Physiol.* **181**, 160–168 (1999).
21. C. B. Bai *et al*., A mouse model for testing remyelinating therapies. *Exp. Neurol.* **283**, 330–340 (2016).
22. K. Magalon *et al*., Olesoxime accelerates myelination and promotes repair in models of demyelination. *Ann. Neurol.* **71**, 213–226 (2012).
23. E. M. Medina-Rodríguez *et al*., Promoting in vivo remyelination with small molecules: A neuroreparative pharmacological treatment for Multiple Sclerosis. *Sci. Rep.* **7**, 43545 (2017).
24. K. Balasubramanyam, V. Swaminathan, A. Ranganathan, T. K. Kundu, Small molecule modulators of histone acetyltransferase p300. *J. Biol. Chem.* **278**, 19134–19140 (2003).
25. M. Hemshekhar, M. Sebastin Santhosh, K. Kemparaju, K. S. Girish, Emerging roles of anacardic acid and its derivatives: A pharmacological overview. *Basic Clin. Pharmacol. Toxicol.* **110**, 122–132 (2012).
26. Z. Hubler *et al*., Accumulation of 8,9-unsaturated sterols drives oligodendrocyte formation and remyelination. *Nature* **560**, 372–376 (2018).
27. F. J. Najm *et al*., Drug-based modulation of endogenous stem cells promotes functional remyelination in vivo. *Nature* **522**, 216–220 (2015).
28. V. de Rosa *et al*., D-Aspartate treatment attenuates myelin damage and stimulates myelin repair. *EMBO Mol. Med.* **11**, e9278 (2019).
29. V. Carriere *et al*., IL-33, the IL-1-like cytokine ligand for ST2 receptor, is a chromatin-associated nuclear factor in vivo. *Proc. Natl. Acad. Sci. U.S.A.* **104**, 282–287 (2007).
30. A. B. Molofsky, A. K. Savage, R. M. Locksley, Interleukin-33 in tissue homeostasis, injury, and inflammation. *Immunity* **42**, 1005–1019 (2015).
31. N. T. Martin, M. U. Martin, Interleukin 33 is a guardian of barriers and a local alarmin. *Nat. Immunol.* **17**, 122–131 (2016).
32. S. P. Gadani, J. T. Walsh, I. Smirnov, J. Zheng, J. Kipnis, The glia-derived alarmin IL-33 orchestrates the immune response and promotes recovery following CNS injury. *Neuron* **85**, 703–709 (2015).
33. D. Shao *et al*., Nuclear IL-33 regulates soluble ST2 receptor and IL-6 expression in primary human arterial endothelial cells and is decreased in idiopathic pulmonary arterial hypertension. *Biochem. Biophys. Res. Commun.* **451**, 8–14 (2014).
34. G. Palmer, C. Gabay, Interleukin-33 biology with potential insights into human diseases. *Nat. Rev. Rheumatol.* **7**, 321–329 (2011).
35. A. M. Miller, Role of IL-33 in inflammation and disease. *J. Inflamm.* **8**, 22 (2011).
36. Y. Xiao *et al*., Interleukin-33 deficiency exacerbated experimental autoimmune encephalomyelitis with an influence on immune cells and glia cells. *Mol. Immunol.* **101**, 550–563 (2018).

37. M. Kurowska-Stolarska *et al*., IL-33 induces antigen-specific IL-5+ T cells and promotes allergic-induced airway inflammation independent of IL-4. *J. Immunol.* **181**, 4780–4790 (2008). Erratum in: *J. Immunol.* **181**, 8170 (2008).
38. S. Mi *et al*., LINGO-1 is a component of the Nogo-66 receptor/p75 signaling complex. *Nat. Neurosci.* **7**, 221–228 (2004).
39. D. Cadavid *et al*.; RENEW Study Investigators, Safety and efficacy of opicinumab in acute optic neuritis (RENEW): A randomised, placebo-controlled, phase 2 trial. *Lancet Neurol.* **16**, 189–199 (2017).
40. D. Cadavid *et al*.; RENEW Study Investigators, Predictors of response to opicinumab in acute optic neuritis. *Ann. Clin. Transl. Neurol.* **5**, 1154–1162 (2018).
41. V. A. Deshmukh *et al*., A regenerative approach to the treatment of multiple sclerosis. *Nature* **502**, 327–332 (2013).
42. B. A. C. Cree *et al*., Clemastine rescues myelination defects and promotes functional recovery in hypoxic brain injury. *Brain* **141**, 85–98 (2018).
43. F. Wang *et al*., Enhancing oligodendrocyte myelination rescues synaptic loss and improves functional recovery after chronic hypoxia. *Neuron* **99**, 689–701.e5 (2018).
44. A. J. Green *et al*., Clemastine fumarate as a remyelinating therapy for multiple sclerosis (ReBUILD): A randomised, controlled, double-blind, crossover trial. *Lancet* **390**, 2481–2489 (2017).
45. C. J. Schwartzbach *et al*., Lesion remyelinating activity of GSK239512 versus placebo in patients with relapsing-remitting multiple sclerosis: A randomised, single-blind, phase II study. *J. Neurol.* **264**, 304–315 (2017).
46. National Research Council, *Guide for the Care and Use of Laboratory Animals*, (National Academies Press, Washington, D.C., 8th Ed., 2011).
47. S. Y. Yao, C. Natarajan, S. Sriram, nNOS mediated mitochondrial injury in LPS stimulated oligodendrocytes. *Mitochondrion* **12**, 336–344 (2012).
48. D. B. McGavern, P. D. Murray, M. Rodriguez, Quantitation of spinal cord demyelination, remyelination, atrophy, and axonal loss in a model of progressive neurologic injury. *J. Neurosci. Res.* **58**, 492–504 (1999).
49. T. Chomiak, B. Hu, What is the optimal value of the g-ratio for myelinated fibers in the rat CNS? A theoretical approach. *PLoS One* **4**, e7754 (2009).